

Delta-doping optimization for high quality *p*-type GaN

C. Bayram, J. L. Pau, R. McClintock, and M. Razeghi^{a)}

Center for Quantum Devices, Department of Electrical Engineering and Computer Science, Northwestern University, Evanston, Illinois 60208, USA

(Received 18 February 2008; accepted 29 August 2008; published online 22 October 2008)

Delta (δ -) doping is studied in order to achieve high quality *p*-type GaN. Atomic force microscopy, x-ray diffraction, photoluminescence, and Hall measurements are performed on the samples to optimize the δ -doping characteristics. The effect of annealing on the electrical, optical, and structural quality is also investigated for different δ -doping parameters. Optimized pulsing conditions result in layers with hole concentrations near 10^{18} cm^{-3} and superior crystal quality compared to conventional *p*-GaN. This material improvement is achieved thanks to the reduction in the Mg activation energy and self-compensation effects in δ -doped *p*-GaN. © 2008 American Institute of Physics. [DOI: 10.1063/1.3000564]

I. INTRODUCTION

Group III-nitrides are of interest for many optoelectronic devices due to their large direct bandgap, which spans from the ultraviolet to the visible spectrum.^{1–3} However, difficulty in realizing *p*-type GaN prevented the realization of devices until the 1990s.⁴ *P*-GaN is a crucial part of III-nitride light-emitting diodes and *p-i-n* photodetectors. Low quality and limited doping of the *p*-type is still one of the biggest problems in realizing high performance nitride based devices.

Standard GaN growth conditions by metalorganic chemical vapor deposition (MOCVD) lead to hole concentrations typically on the order of $(1-4) \times 10^{17} \text{ cm}^{-3}$.^{4,5} However, for many devices, it is desirable to obtain higher hole concentrations. Using higher growth pressures and lower temperatures can enable higher hole concentrations.^{6,7} However, higher growth pressures and lower growth temperatures lead to material degradation.⁶ In addition, this approach is limited by self-compensation and at best obtains concentrations in the range of $(5-14) \times 10^{17} \text{ cm}^{-3}$.^{7,8} Self-compensation is attributed to nitrogen vacancy complexes in *p*-GaN.⁹ Due to the motion of the Fermi level, nitrogen vacancies are expected to have a major impact on *p*-type GaN.⁶ However, with higher ammonia partial pressures during growth and careful post annealing, the nitrogen vacancy (a triple donor) density can be minimized.¹⁰ The hole concentration in MOCVD-grown *p*-type GaN is also limited by the formation of the Mg-H complexes, which inhibit the ionization of Mg acceptors. In order to depassivate these Mg-H complexes, low-energy electron beam irradiation⁴ and thermal annealing⁵ have been used traditionally.

Delta (δ -) doping has been proposed¹¹ and shown to improve hole concentrations in II-VI wide-band-gap semiconductors (such as ZnSe) in which *p*-type doping is difficult.¹² Recently, this approach has been applied to *p*-type (Al)GaN and shown to improve hole concentration without severe degradation of the material quality,^{7,13,14} this has led to the use of δ -doping in the realization of high performance nitride devices.^{15,16}

In this work, *p*-type GaN δ -doping parameters such as nitridation time, GaN period, and Mg flow time are investigated, while maintaining lower pressures and higher temperatures for higher material quality. In addition, electrical, optical, and structural measurements are conducted both before and after annealing to address the Mg-H complex depassivation and self-compensation dependency on the δ -doping parameters.

II. EXPERIMENT

The samples are grown using an AIXTRON 200/4-HT horizontal flow, low pressure MOCVD reactor. Trimethylgallium (TMGa), trimethylaluminum, and bis(cyclopentadienyl)magnesium (DcpMg) are the metal-organic cation precursors for Ga, Al, and Mg, respectively; hydrogen is used as the carrier gas. Ammonia (NH₃) is used as the nitrogen source. All growth is performed at a pressure of 100 mbar and a temperature of 1100 °C. The GaN growth rate is 27 nm/min under these conditions, and the DcpMg flow rate is 236 nmol/min.

For the sake of comparison, GaN samples were grown on AlN/low-temperature (LT)-AlN buffer/sapphire templates and directly on LT-GaN buffer/sapphire substrates. Table I shows the electrical and structural properties of GaN layers deposited on both templates. Higher mobility and lower x-ray full-width-at-half-maximum (FWHM) indicates the superior quality of GaN on AlN/LT-AlN buffer/sapphire templates over on LT-GaN buffer/sapphire ones. Atomic force microscopy (AFM) also demonstrates much smoother surface with clear evidence of atomic steps for GaN/AlN/sapphire (Fig. 1). The high resistivity of AlN and high quality of regrown GaN make AlN a good template for *p*-GaN doping studies. Thus, AlN/sapphire templates are used in subsequent experiments.

For *p*-type doping studies, 250-nm-thick *p*-GaN (either conventionally, or delta-doped) is grown on a 600-nm-thick AlN/LT-AlN buffer/sapphire template. Surface quality by AFM, crystalline quality by x-ray diffraction (XRD), electrical properties by Hall measurement, and optical characteristics by photoluminescence (PL) are investigated. As-grown

^{a)}Electronic mail: razeghi@eecs.northwestern.edu.

TABLE I. Properties of unintentionally doped GaN on LT-GaN buffer/sapphire and AlN/LT-AlN buffer/sapphire.

Unintentionally doped GaN on	Background carrier concentration (cm ⁻³)	Mobility (cm ² /V s)	(002) FWHM (arc sec)	rms surface roughness (Å)
LT-GaN buffer/sapphire	-1.95×10^{17}	188	380	2.14
AlN/LT-AlN buffer/sapphire	-4.25×10^{16}	541	220	1.74

samples exhibit semi-insulating properties. Rapid thermal annealing was conducted for Mg activation using previously optimized conditions of 1000 °C under N₂ for 30 s.

The δ -doping profile is implemented as shown in Fig. 2: (I) a specific thickness of GaN is deposited normally to grow the GaN period, (II) the TMGa flow is then stopped and the crystal surface is allowed to nitridize, and finally (III) the DcpMg flow is introduced for a specific Mg flow time. The dopant flow is then stopped and TMGa flow resumed so that the cycle can repeat as the next GaN period is grown.¹⁷ The Mg dopants are only slightly expected to diffuse through GaN during growth and annealing¹⁸ whereas the hole concentration is expected to be uniformly distributed.¹⁶

III. RESULT AND DISCUSSION

The nitridation time is varied from 15 to 120 s. No significant changes in the hole concentration are observed (<5%). Thus, a nitridation time of 30 s is used for the rest of the study to ensure a stable GaN surface before the Mg flow is introduced.

In order to optimize the hole concentration and material quality of the δ -doped *p*-GaN, first the Mg flow time is varied from 15 to 60 s. The effect of Mg flow time on hole concentration, resistivity, and mobility is shown in Fig. 3(a) for annealed samples. The high hole concentration achieved by δ -doping suggests successful depassivation of the Mg-H complexes and reduction in self-compensating effects after annealing.^{9,19,20} Keeping the GaN period at 10 nm, with increasing Mg flow time, hole concentration increases and mo-

bility decreases. The higher hole concentration compensates the mobility decrease leading to a reduction in resistivity with increasing Mg flow time. For comparison, conventional *p*-GaN is also grown using the same growth conditions by supplying TMGa and DcpMg together. The results of the conventional doping are indicated as dashed-levels at each axis (Fig. 3). Comparing the δ -doping to the conventional doping, around two orders of magnitude higher doping is achieved under the same growth conditions, with four times lower resistivity.

In order to assess the structural properties, open detector omega/2theta (002) XRD scans are performed before and after annealing. The XRD FWHM is plotted with respect to the Mg flow time in Fig. 3(b). An increase in the FWHM in Fig. 3(b) suggests increase in crystal imperfections.²¹ Increasing nonsubstitutional Mg incorporation, heterogeneous strain or threading dislocations may contribute to broaden the (002) reflection as Mg flow increases. Similar to conventionally doped *p*-GaN, the annealing decreases the FWHM of δ -doped *p*-GaN for the highest hole concentrations, as seen in Fig. 3(b).

Then, Mg flow time is fixed at 38 s, and the GaN period is varied—this Mg flow time leads to a suitable hole concentration for observing hole concentration progress with the change in other δ -doping parameters. The effect of GaN period on hole concentration is shown in Fig. 4(a). It is seen that for a 10 nm period the resistivity is minimized, and hole concentration is maximized (2×10^{17} cm⁻³). Figure 4(b) shows the omega/2theta (002) XRD FWHM versus GaN pe-

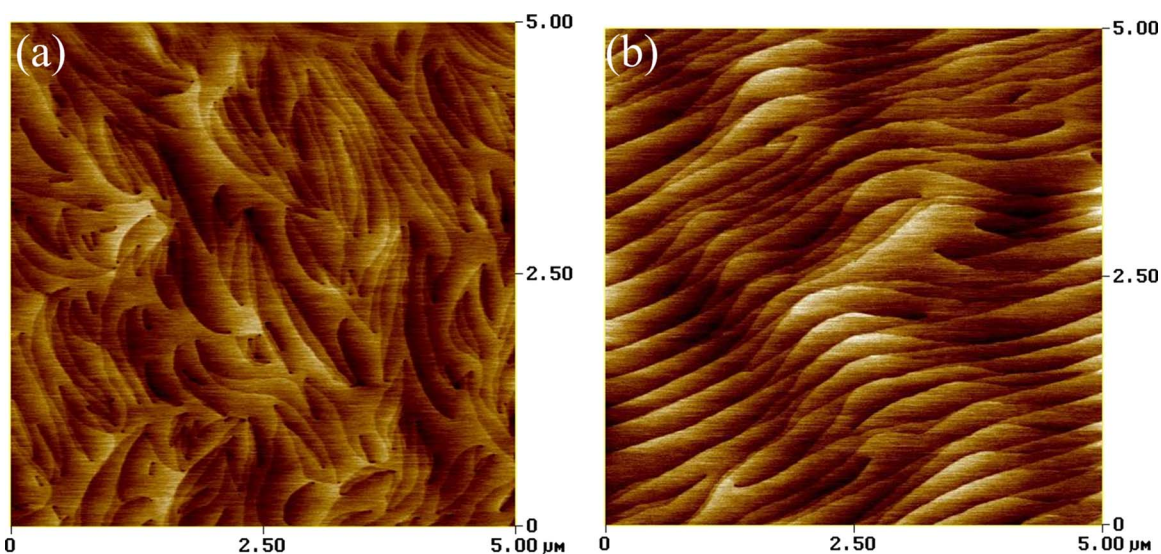


FIG. 1. (Color online) ($5 \times 5 \mu\text{m}^2$) AFM images of *i*-GaN (a) on LT-GaN buffer/sapphire and (b) on AlN/LT-AlN buffer/sapphire. Both images have a height scale of 2 nm.

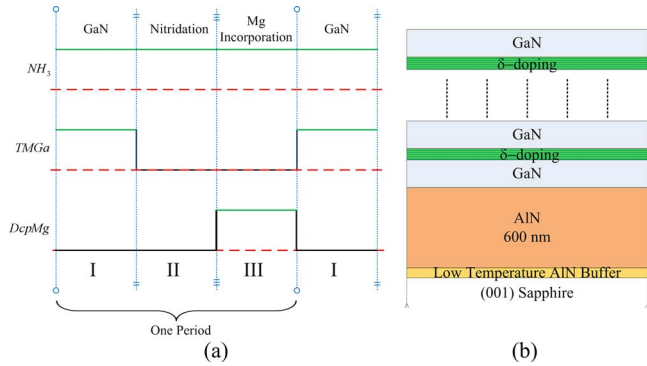


FIG. 2. (Color online) (a) δ -doping profile implementation. (b) Side view of the δ -doped p -GaN structure.

riod. For the longer period, annealing decreases the FWHM, whereas for the shorter period, annealing increases the FWHM; this suggests that different mechanisms are dominant in each region, both of which require analysis.

In conventionally doped p -GaN or δ -doped p -GaN with hole concentrations in the range of 10^{17} cm^{-3} , we observe a decrease in XRD FWHM via annealing. This could be due to successful depassivation of the Mg–H complexes and lack of self-compensation centers. On the other hand, samples with the smallest period seem to show strong self-compensating effect. The decrease in period, as Mg flow time is constant, increases average Mg concentration. This results in movement of the Fermi level leading to more nitrogen vacancy (V_N).⁶ Increase in both Mg dopant and V_N concentration lead to compensation effects (formation of V_N – Mg_{Ga} complexes) identified by lower hole concentration and blue line PL. Thus, compensation mechanism is known to be dominant for this sample and may play a role in the broadening of the XRD FWHM observed in Fig. 4(b).

Room temperature (RT) PL of annealed δ -doped p -GaN with different GaN periods is shown in Fig. 5(a). For the shortest GaN period, the PL spectrum is dominated by a broad emission band centered at 2.91 eV. This band has been previously observed in conventional p -GaN and has been

attributed to V_N – Mg_{Ga} complexes showing donor-acceptor-pair (DAP) characteristics.²² For longer GaN periods, the spectrum begins to be dominated by 3.41 eV GaN band-edge emission and by a secondary 3.29 eV line. The optimized GaN period sample in our work shows a significant optical emission at 3.29 eV. The 3.29 eV line is believed to be due to transitions between the conduction band and the Mg shallow acceptor level. Hence, the observance of the Mg shallow acceptor level at RT indicates successful Mg activation. Similar line energies have been observed at 10 K in other studies.^{14,23}

The effect of annealing on the optical transitions is shown in Fig. 5(b). After annealing, the deep Mg levels emitting in the broad range from 370 to 450 nm disappears and GaN and shallow Mg acceptor levels appear indicating successful Mg–H complex depassivation and reduction in self-compensation effects. For the shortest GaN period, no such transition occurs, and only DAP transition centered at 2.91 eV is observed with slight intensity increase after annealing.

Correlating this with the Hall measurements, x ray and PL data suggest that by δ -doping optimization, hole concentrations on the order of 10^{18} cm^{-3} can be achieved and self-compensation effects can be reduced. This is due to the material improvement and to δ -doping's ability to decrease the acceptor activation energy. It is known that the activation energy (E_A) of dopants is affected by the average distance between ionized acceptors.^{24–26} An overlapping of the Coulomb potentials of the ionized acceptors should decrease the Mg activation energy.²⁶ By concentrating the Mg dopants into a very thin layer by using the δ -doping technique, the acceptor activation energy is expected to decrease obeying

$$\Delta E(N_A^-) = \Delta E_{A,0} - f \frac{q^2}{4\pi\epsilon_S} (N_A^-)^{1/3}, \quad (1)$$

where N_A^- is the ionized Mg concentration and $\Delta E(N_A^-)$ is the activation energy at this concentration, $\Delta E_{A,0}$ is the activation energy for a very low acceptor concentration (taken to

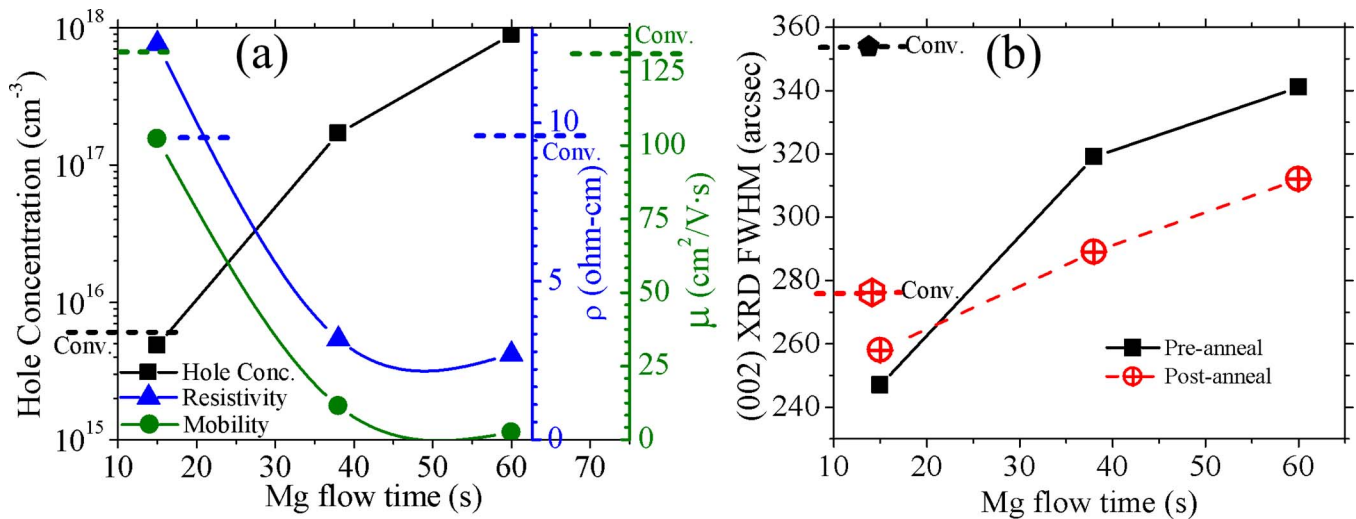


FIG. 3. (Color online) (a) Effect of the Mg flow time on hole concentration, resistivity (ρ), and mobility (μ). (b) Effect of Mg flow time and annealing on (002) (ω / 2θ) XRD FWHM. GaN period is 10 nm for both graphs. The results of the conventional doping are indicated as dashed-levels at each axis.

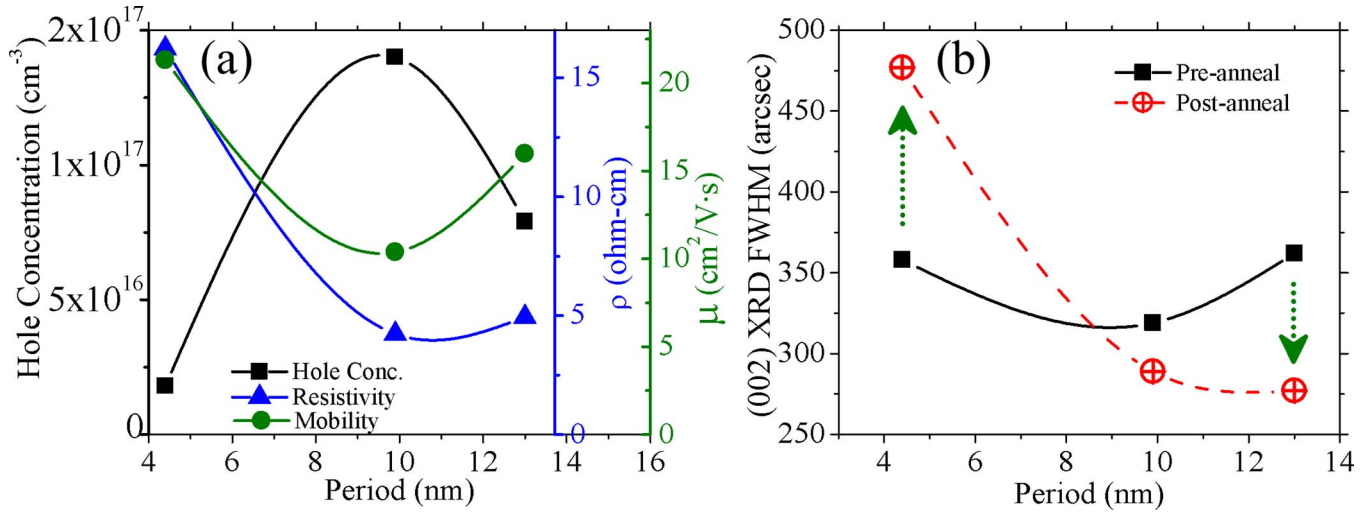


FIG. 4. (Color online) (a) Effect of GaN period on hole concentration, resistivity (ρ), and mobility (μ). (b) Effect of GaN period and annealing on (002) (ω /2 θ) XRD FWHM. Mg flow time is 38 s for both graphs.

be 230 meV), f is a geometric factor (given by $\Gamma(2/3)$ ($4\pi/3$)^{1/3}) and describes the probability of finding another ionized acceptor in the neighborhood of an ionized acceptor, and ϵ_S is the dielectric constant for GaN.^{8,25,26} Taking the hole concentration as N_A^- in Eq. (1), the activation energies in δ -doped p -GaN are calculated and plotted in Fig. 6.

The activation energies are plotted as a function of Mg flow times in Fig. 6(a). The activation energy decreases linearly with increasing Mg flow time. Dense packing of Mg acceptors results in a lowering of the Mg activation energy as expected. The dependence of the activation energy on the GaN period, for a constant Mg flow time (of 38 s), is shown in Fig. 6(b). For longer periods the activation energy is almost constant at ~ 164 meV, whereas for the shortest period it is ~ 230 meV. This should be due to the increase in the period of the conduction band and valence band oscillations formed by δ -doping.^{11,17} In summary, the Mg activation energy is expected to decrease linearly with the increase in Mg

flow time. The activation energy becomes less dependent on GaN period for larger periods.

IV. CONCLUSION

P -type doping in the near 10^{18} cm⁻³ range using a δ -doping technique is achieved by systematically optimizing the growth conditions while preserving the material quality. Mg flow time is shown to increase the hole concentration. The GaN period is determined to be crucial for successful Mg-H depassivation and lowering self-compensation effects via annealing. Successful annealing results in a smaller XRD FWHM and a RT Mg-level luminescence at 3.29 eV.

The doping enhancement in the case of δ -doped p -GaN is due to (1) the decrease in Mg activation energy due to dense packing of Mg dopants and (2) lower self-compensation effects. This technique could be particularly

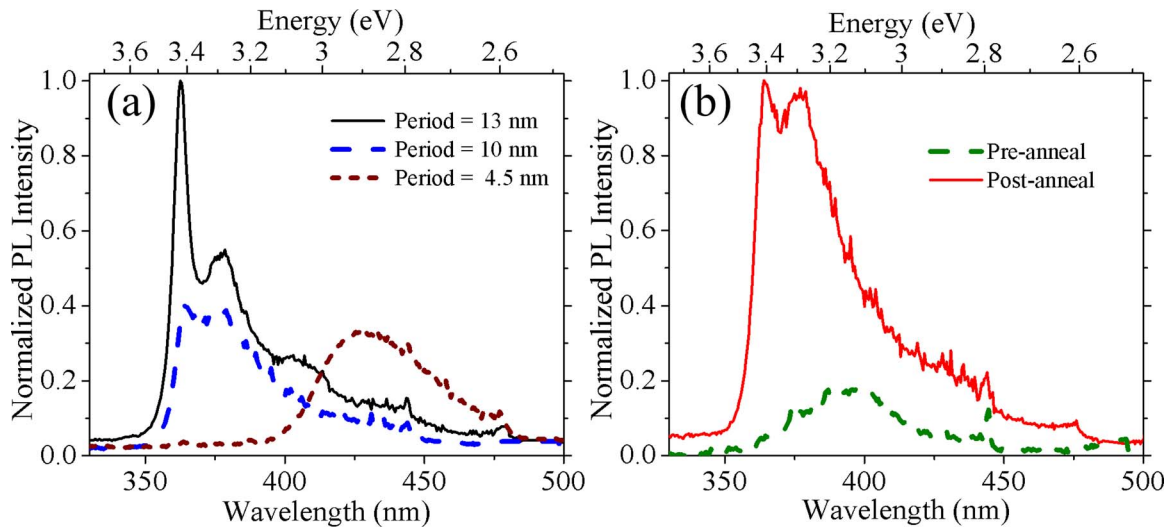


FIG. 5. (Color online) PL study at RT: (a) effect of GaN period on PL and (b) effect of annealing on 10 nm period samples. Mg flow time is 38 s for both graphs.

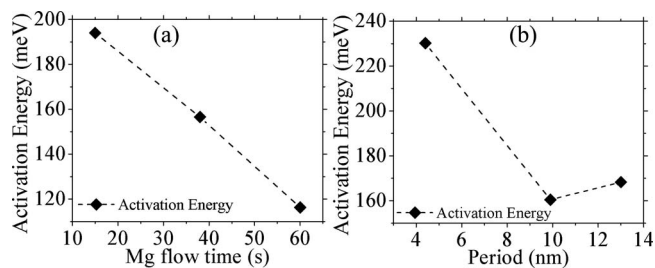


FIG. 6. (a) Effect of Mg flow time on Mg activation energy (GaN period = 10 nm). (b) Effect of GaN period on Mg activation energy (Mg flow time = 38 s).

beneficial for *p*-AlGaIn where low pressures are required for avoiding parasitic reactions and where high temperatures are required for high quality.

ACKNOWLEDGMENTS

The authors thank D. Hoffman from the Center for Quantum Devices for valuable support during electrical measurements. The authors also acknowledge the Fulbright Association and the Spanish Ministry of Education and Science for supporting one of the authors (J.L.P.).

¹P. Kung, A. Yasan, R. McClintock, S. R. Darvish, K. Mi, and M. Razeghi, *Proc. SPIE* **4650**, 199 (2002).

²M. Razeghi, *Proc. IEEE* **90**, 1006 (2002).

³O. Ambacher, *J. Phys. D* **31**, 2653 (1998).

⁴H. Amano, M. Kito, K. Hiramatsu, and I. Akasaki, *Jpn. J. Appl. Phys., Part 2* **28**, L2112 (1989).

⁵S. Nakamura, T. Mukai, M. Senoh, and N. Iwasa, *Jpn. J. Appl. Phys., Part 2* **31**, L139 (1992).

⁶P. Kozodoy, S. Keller, S. P. DenBaars, and U. K. Mishra, *J. Cryst. Growth* **195**, 265 (1998).

⁷T. Li, C. Simbrunner, M. Wegscheider, A. Navarro-Quezada, M. Quast, K. Schmidegg, and A. Bonanni, *J. Cryst. Growth* **310**, 13 (2008).

⁸U. Kaufmann, P. Scholetter, H. Obloh, K. Kohler, and M. Maier, *Phys. Rev. B* **62**, 10867 (2000).

⁹S. Hautakangas, V. Ranki, I. Makkonen, M. J. Puska, K. Saarinen, L. Lizzkay, D. Seghier, H. P. Gislason, J. A. Freitas, Jr., R. L. Henry, X. Xu, and D. C. Look, *Physica B (Amsterdam)* **376–377**, 424 (2006).

¹⁰S. Hautakangas, K. Saarinen, L. Lizzkay, J. A. Freitas, Jr., and R. L. Henry, *Phys. Rev. B* **72**, 165303 (2005).

¹¹F. Schubert, *J. Vac. Sci. Technol. A* **8**, 2980 (1990), Part 2.

¹²S. P. Guo, W. Lin, X. Zhou, M. C. Tamargo, C. Tian, I. Kuskovsky, and G. F. Neumark, *J. Appl. Phys.* **90**, 1725 (2001).

¹³H. Wang, J. Liu, N. Niu, G. Shen, and S. Zhang, *J. Cryst. Growth* **304**, 7 (2007).

¹⁴M. L. Nakarmi, K. H. Kim, J. Li, J. Y. Lin, and H. X. Jiang, *Appl. Phys. Lett.* **82**, 3041 (2003).

¹⁵K. H. Kim, J. Li, S. X. Jin, J. Y. Lin, and H. X. Jiang, *Appl. Phys. Lett.* **83**, 566 (2003).

¹⁶C. Bayram, J. L. Pau, R. McClintock, and M. Razeghi, *Appl. Phys. Lett.* **92**, 241103 (2008).

¹⁷F. Schubert, *Doping in III-V Semiconductors* (Cambridge, New York, 1993), pp. 433–471.

¹⁸C. Simbrunner, M. Wegscheider, M. Quast, T. Li, A. Navarro-Quezada, H. Sitter, and A. Bonanni, *Appl. Phys. Lett.* **90**, 142108 (2007).

¹⁹S. Hautakangas, K. Saarinen, L. Lizzkay, J. A. Freitas, Jr., and R. L. Henry, *Phys. Rev. B* **72**, 165303 (2005).

²⁰J. Neugebauer and C. G. Van de Walle, *Phys. Rev. Lett.* **75**, 4452 (1995).

²¹T. Metzger, R. Höppler, E. Born, O. Ambacher, M. Stutzmann, R. Stömmmer, M. Schuster, H. Göbel, S. Christiansen, M. Albrecht, and H. P. Strunk, *Philos. Mag. A* **77**, 1013 (1998).

²²U. Kaufmann, M. Kunzer, M. Maier, H. Obloh, A. Ramakrishnan, B. Santic, and P. Scholetter, *Appl. Phys. Lett.* **72**, 1326 (1998).

²³M. Smith, G. D. Chen, J. Y. Lin, H. X. Jiang, A. Salvador, B. N. Sverdlov, A. Botchkarev, H. Morkoc, and B. Goldenberg, *Appl. Phys. Lett.* **68**, 1883 (1996).

²⁴P. P. Debye and E. M. Conwell, *Phys. Rev.* **93**, 693 (1954).

²⁵P. Kozodoy, H. Xing, S. P. Denbaars, U. K. Mishra, A. Saxler, R. Perrin, S. Elhamri, and W. C. Mitchel, *J. Appl. Phys.* **87**, 1832 (2000).

²⁶W. Gotz, R. S. Kern, C. H. Chen, H. Liu, D. A. Steigerwald, and R. M. Fletcher, *Mater. Sci. Eng., B* **59**, 211 (1999).